6ICEGE
6th International Conference on Earthquake Geotechnical Engineering
1-4 November 2015
Christchurch, New Zealand

Lateral spreading: evidence and interpretation from the 2010-2011 Christchurch earthquakes

M. Cubrinovski[1], K. Robinson[2]

ABSTRACT

In the 2010-2011 Canterbury earthquakes widespread liquefaction occurred over nearly half of the urban area of Christchurch. The most severe damage to buildings and infrastructure was often associated with lateral spreading and consequent large ground distortion and permanent ground displacements. This paper presents results, analysis and interpretation of lateral spreads using measurements from detailed ground surveying at a large number of locations along the Avon River. Classification of lateral spreads based on the magnitude and spatial distribution of permanent ground displacements is first presented, and then key characteristics of soil layers and ground conditions associated with different classes of lateral spreads are identified and discussed. Evidence of both global effects from topographic features and local effects related to thicknesses and continuity of critical layers is presented highlighting the need for a systematic approach in the engineering evaluation of lateral spreading in which particular attention should be given to factors governing lateral spreading.

Introduction

In the period between September 2010 and December 2011, Christchurch (population: ~ 380,000; area: ~ 450 km^2) was hit by a series of strong earthquakes known as the Canterbury Earthquake Sequence (CES). The sequence included four significant events with magnitudes M_w 5.9 to 7.1 and causative faults either in proximity to or within the city boundaries thus generating very strong ground motions and seismic demand throughout Christchurch. The earthquakes caused tremendous damage and total economic loss of approximately $30 billion dollars (NZD). The second earthquake in the sequence, the 22 February 2011 (Christchurch earthquake) was the most devastating; it caused 185 fatalities, mostly due to the collapse of two multi-storey reinforced concrete buildings.

The earthquakes had significant geotechnical features both in the extent and severity of damage. Geotechnical failures and associated damage were widespread across the city, and were the most prominent damage feature outside the Central Business District (CBD). All four major events triggered extensive liquefaction particularly in the eastern suburbs of Christchurch. The Christchurch earthquake caused widespread liquefaction over nearly half of the city area while rock falls and slope instabilities affected residential areas in the Port Hills, along the south-east

[1]Professor, Department of Civil and Natural Resources Engineering, University of Canterbury, Christchurch, New Zealand, misko.cubrinovski@canterbury.ac.nz
[2]PhD Student, Department of Civil and Natural Resources Engineering, University of Canterbury, Christchurch, New Zealand, kelly.robinson@pg.canterbury.ac.nz

perimeter of the city. The extent of the liquefaction caused by the Christchurch earthquake is depicted in Figure 1. The liquefaction affected nearly 60,000 residential buildings and properties, out of which 20,000 were severely affected and about 8,000 properties were abandoned because the excessive damage caused by liquefaction and lateral spreading was deemed uneconomical for reinstatement of residential land. Liquefaction and lateral spreading also caused heavy damage to CBD buildings, roads, bridges, and buried pipe networks of potable and wastewater systems of Christchurch. Typical examples of spreading-induced damage to buildings and infrastructure are shown in Figure 2.

This paper focuses on lateral spreading, and presents results from a comprehensive study in which characteristics of lateral spreads were investigated using the so-called *ground surveying* method (Robinson, 2015). First, a large number of detailed measurements at locations affected by lateral spreading are used to identify magnitudes and distribution patterns of permanent ground displacements due to lateral spreading. Next, lateral spreads are classified based on their manifestation features, and geotechnical analysis and interpretation are used to examine characteristics of soil layers and ground conditions in relation to different classes of lateral spreads. The key objective of this evaluation is to identify critical factors that influence and govern lateral spreading.

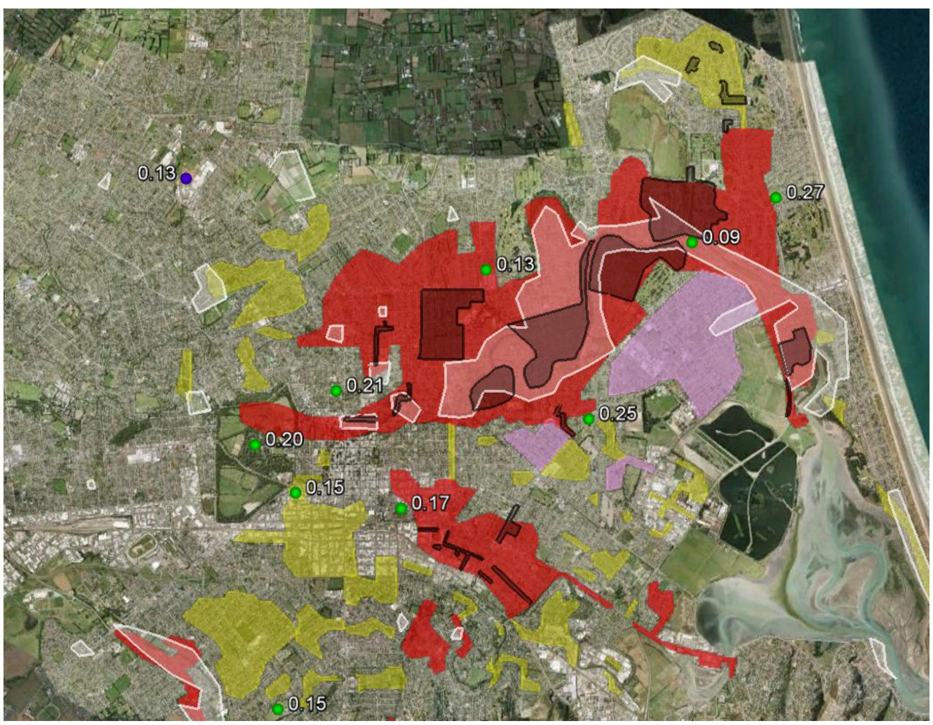

Figure 1. Liquefaction maps indicating areas of observed liquefaction in the 4 September 2010 (white contours), 22 February 2011 (red, yellow, magenta areas), and 13 June 2011 (black contours) earthquakes; normalized cyclic stress ratios at water table depth, CSR7.5(wt), which were calculated using the recorded geometric mean peak ground accelerations and respective earthquake moment magnitudes are also shown (green symbols indicate strong motion stations where the 22 February 2011 produced the highest CSR7.5(wt) value whereas the 4 September 2010 earthquake produced the highest CSR7.5(wt) value at the SMS depicted with blue symbols)

Local Geology and Ground Conditions

The Canterbury Plains are composed of complex alluvial fans deposited by eastward-flowing rivers draining the Southern Alps and discharging into Pegasus Bay on the Pacific Coast. Christchurch lies along the eastern extent of the Canterbury Plains, just north of the Banks Peninsula, the eroded remnant of the extinct Lyttelton Volcano, comprised of weathered basalt and Pleistocene loess. Originally, the site of Christchurch was mainly swamp lying behind beach dune sand, estuaries and lagoons, with gravel, sand, and silt of river channel and flood deposits of the coastal Waimakariri River flood plain (Brown and Weeber, 1992). The dominant features of present day Christchurch are the Avon and Heathcote Rivers, which originate from springs in western Christchurch, meander through the city and discharge in the Avon-Heathcote Estuary.

Approximately 6,500 years ago the coastline was near the western edge of the present-day CBD. The shallow subsurface in the eastern parts of Christchurch comprises of coastal swamp deposits of sands, silts, some clayey soils and peat (Christchurch Formation). In the western Christchurch, the Springston formation of alluvial gravels, sands and silts is prevalent. The water table to the east of the CBD is generally within 1.0 m to 1.5 m of the ground surface (CGD, 2014), and shallow soils within the top 10 metres are less than 4,000 years old, and some are only few hundred years old (Brown and Weeber, 1992; Cubrinovski and McCahon, 2011).

The depositional environment, soil composition, young age of the deposits, low in situ densities and shallow water table of Christchurch soils all point towards a high liquefaction potential of these soils, which was amply demonstrated during the Canterbury earthquakes. A couple of additional factors need to be emphasized for the Christchurch soils. Typically there is a substantial spatial variability of soils both vertically and horizontally, and also soils of high liquefaction potential include clean sands, and sand-silt mixtures with fines content of 10 % to 100 % involving predominantly non-plastic and low plasticity fines.

Figure 2. Spreading-induced damage to roads, residential and CBD buildings (after Cubrinovski et al., 2012)

General Observations on Lateral Spreading in Christchurch

The widespread liquefaction triggered by the CES events was accompanied by lateral spreading, which typically occurred in areas along waterways (rivers, streams, estuaries, marshland). The spreading was manifested by large permanent ground displacements towards the waterway, and associated settlement and subsidence in the area affected by spreading. Large ground distortion, ground cracks and fissures, and vertical offsets were observed in areas affected by severe spreading. Generally, largest cracks, ground distortion and magnitudes of permanent ground displacements were observed near the river banks. Maximum lateral ground displacements at the river banks ranged from several tens of centimetres up to 1 m, 2 m or even 3 m. These features of lateral spreading are depicted in Figure 3 where the location and width of cracks and fissures observed on the ground surface are shown (CGD, 2013). These data were obtained using field land damage inspections in the assessment of liquefaction and spreading-induced damage to residential properties by Tonkin and Taylor (T&T) and EQC engineers. There is clear concentration of cracks and fissures along the banks of the Avon River. A close inspection also shows that many of the cracks run parallel to the river indicating that they are associated with lateral movement of the ground towards the river. It is also evident, however, that some cracks are concentrated at ridges and higher elevation areas, both near and away from the river, providing clear evidence that topographic features also played an important role in 'driving' and manifestation of lateral spreading. As will be elaborated later on, the ground slopes in the vicinity of the river banks are very small, but despite this fact, a slumping mode of deformation involving settlement of the ridges and lateral movement in the downslope direction is apparent for many of the areas with even small elevation differences. The above shows clear governing effects of free face at waterways and topography on the driving mechanism and manifestation of lateral spreading.

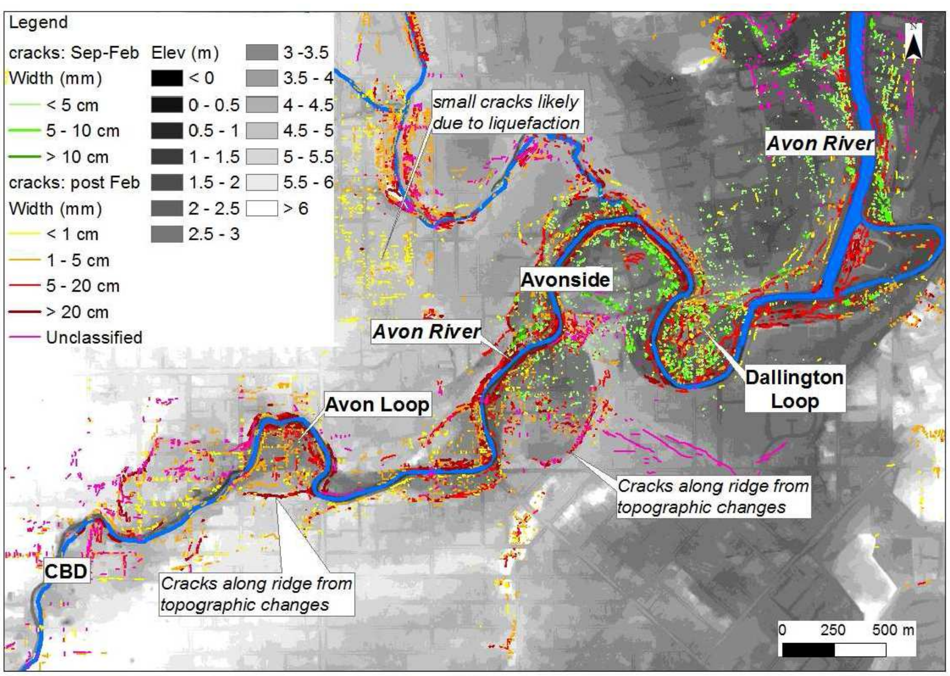

Figure 3. Ground cracks identified in field inspections (CGD, 2013)

After the Canterbury earthquakes, generally two types of investigations of lateral spreading were performed. Local measurements, using field inspections and surveys, and global aerial surveys using LiDAR, aerial photography and satellite images. The field inspections, which are the focus of this study, are based on simple ground surveying technics in which ground cracks are first measured at a particular location (site), and permanent ground displacements are then estimated by superposition of the widths of the cracks measured at site. When employing this technique, one quickly realizes that lateral spreading manifestation is highly non-uniform showing considerable spatial variability on a local scale. In any case, this type of investigations focus on local features of lateral spreading, at a particular location, and are typically performed within a zone from the river banks to about 200 m distance from the river.

High quality LiDAR data (and to a lesser extent aerial photography) were also obtained after each of the four major CES events. Figure 4 shows summary interpretation of permanent lateral ground displacements obtained from pre-event (pre 4 September 2010) and post-event (post 22 February 2011) LiDAR data for the stretch along the Avon River from the CBD to Avondale. The coloured vectors indicate both the magnitude and directions of ground displacements, whereas the black arrows show the predominant direction of spreading for a given area. Note that vectors with displacement magnitudes smaller than 0.30 m have been removed since they were considered as 'noise' and not reliable in view of the estimated horizontal accuracy of LiDAR points of about 0.50 m (T&T, 2015 – private communication). Also, Figure 4 shows in the background ground cracks and elevation above reference datum point (MSL) thus providing supporting information for the interpretation of the spreading movement and their association with the free face of the river channel or/and topographic features. Clearly, the LiDAR data depict and quantify global patterns of movement, which are impossible to recognize in local ground surveying. These data show movements predominantly towards the Avon River, but also few vectors pointing away from the river due to topographic influence on lateral spreading.

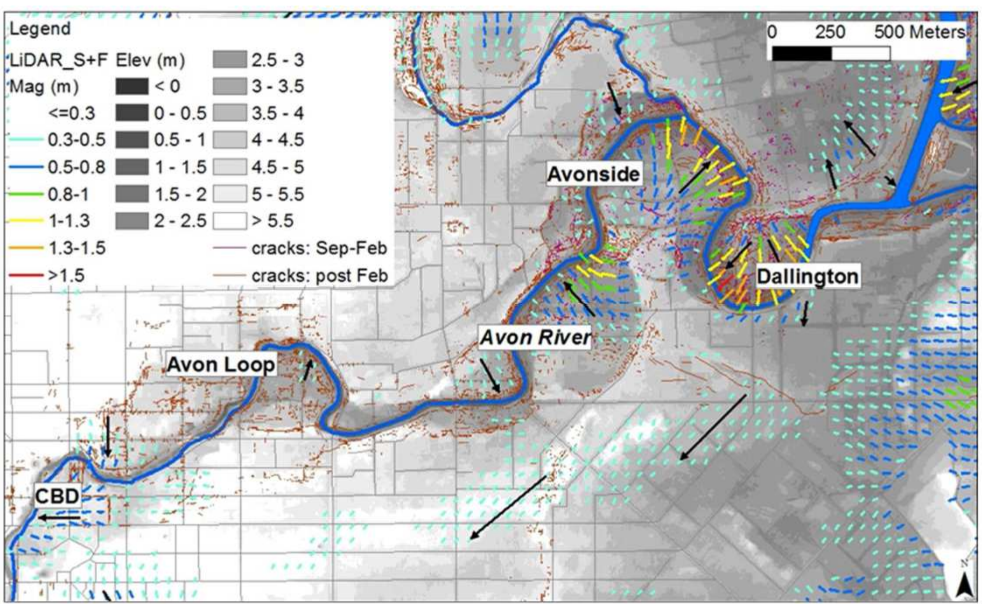

Figure 4. Vectors of permanent lateral ground displacement estimated based on LiDAR data (CGD, 2013)

Characterization of lateral spreads is a very challenging task because spreading is affected by a complex interplay of various local and global factors. In this context, it is important to understand the differences between local and global surveying methods of lateral spreading including both strengths and weaknesses of each of the methods before attempting any comparison of ground displacements estimated from different methods. In fact, these methods often depict different features of lateral spreading, which are dominated either by local ground characteristics or global features. Since both types of influence are important to properly interpret spreads and quantify consequent ground displacement, it is essential to employ these methods as complementary tools in the assessment and interpretation of lateral spreading. This was the approach taken in this study, which is based on local ground surveying measurement of lateral spreading displacements, but also included the use of LiDAR data in the interpretation of topographic effects and differentiation (wherever possible) between topographic and free-face effects.

Characteristics of Lateral Spreading Displacements

Ground Surveying Measurements and Their Interpretation

Following the Darfield (Sep2010) and Christchurch (Feb2011) earthquakes, detailed measurements of lateral spreading were conducted along specific transects running perpendicular to waterways at 126 locations. In performing these measurements, first transect locations were selected involving a wide range of lateral spreading effects from no or small ground displacements to moderate and large permanent spreading displacements. These transects generally run perpendicular to the waterway. In the field, cracks on the ground surface were identified first along the transect. For each crack, the location of the crack (its distance from the waterway) was geotagged, and then the width of the crack and vertical offset were measured and recorded. By superimposing the recorded widths of cracks along the transect, an estimate for the magnitude of lateral ground displacement could be made including its distribution along the length of the transect. In this way, both lateral and vertical ground displacements were estimated. The employed procedure generally followed the approach used by Ishihara et al. (1997), and is described in detail in Robinson (2015).

Figure 5 shows typical results of the 'ground surveying' measurements at one of the transects. The top plot shows estimated permanent horizontal ground displacements and their distribution with the distance from the waterway, based on the field measurements, while the lower plot shows a cross section depicting the general ground slope along the transect, depth to the water table and height of the river channel at the measurement location. In this method, ground cracks were generally measured within a zone of about 150 m to 200 m from the river, because, in most of the cases, there wasn't evidence of spreading-induced ground cracks beyond such distances. In essence, the method provides means for quantifying the effects of spreading at a local level including details of crack distribution, vertical offsets and lateral stretch (and associated equivalent strains). Importantly, the method allows for quantification of both maximum magnitude of permanent ground displacements and spatial distribution of ground displacements. These in turn allow for assessment of differential ground movements producing lateral stretch and vertical offsets (differential settlements) which are of principal concern in the engineering evaluation of lateral spreading effects on buildings and infrastructure. Rigorous comparisons of lateral ground displacements estimated using ground surveying measurements, as above, and alternative methods such as local measurements using geodetic surveying, and global surveys using LiDAR and aerial photography were also performed (Robinson, 2015). These comparisons generally confirmed reasonable levels of agreement between spreading displacements obtained using different methods of surveying. By and large, LiDAR showed similar or larger magnitudes of absolute ground displacements as compared to those estimated based on local ground surveying employed in this study. However, LiDAR showed similar or smaller magnitudes of relative ground displacements (within the length of the transect, i.e. in relation to the reference point at the end of the transect) than those estimated from local ground surveying measurements. These outcomes appear consistent with the different focus on local and global spreading features of different surveying methods, and once again emphasise the need to concurrently use local and global surveying methods in the characterization of lateral spreads.

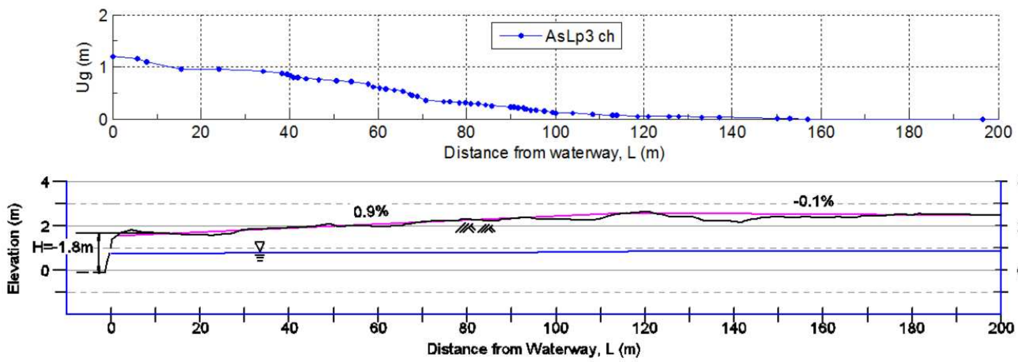

Figure 5. Characteristic data on permanent horizontal displacements obtained from ground surveying, and cross section along one of the transects (Robinson, 2015)

Lateral Spreading Along the Avon River

Measurement Locations and Characteristics of Areas Affected by Spreading

The field surveys were performed predominantly along the Avon River, but also in Kaiapoi and Spencerville (after the Darfield event), and along the Heathcote River (after the February event). In this paper we will examine and illustrate important features of lateral spreads using the data obtained along the Avon River at the transect locations indicated in Figure 6. The investigated sites are distributed along the Avon River from the CBD to the estuary. Red solid lines indicate transects at which measurements were conducted after the Darfield earthquake (i.e. after 4 September 2010, but before 22 February 2011), while blue lines indicate locations of transects along which measurements were conducted after the 22 February 2011 earthquake. Hence, the measurements at the latter locations provide cumulative spreading displacements due to both Darfield and Christchurch earthquakes. At 14 locations measurements were performed both after the Darfield and February events (marked with yellow symbols as ‘Repeat’ transects). Data from these repeat measurements indicate that spreading displacements due to the February 2011 event were generally similar to or greater than the displacements caused by the Darfield 2010 earthquake.

General characteristics of the river channel geometry (free face conditions), slope of the ground surface (topographic features) and peak ground accelerations (seismic demand) along the investigated transects are summarized in Table 1. The height of the river channel is mostly in the range between 2.0 m and 4.0 m, while the width of the channel is largely in the range between 20 m and 40 m. The width and height of the Avon River channel increase from the CBD towards the Avon-Heathcote Estuary. Hence, the lower numbers reported in the table are representative for the river channel characteristics at the CBD, while higher values represent the geometry of the river close to the estuary.

The slope of the ground surface within the zone affected by spreading (i.e. within approximately 150 m from the Avon River) is very small or negligible. For half of the transects shown in Figure 6, the average (global) ground slope was less than 1%, while for 90 % of the transects the ground slope was less than 2%. These river channel geometry and mild ground slopes are important to keep in mind when interpreting the observed ground displacements of the lateral spreads.

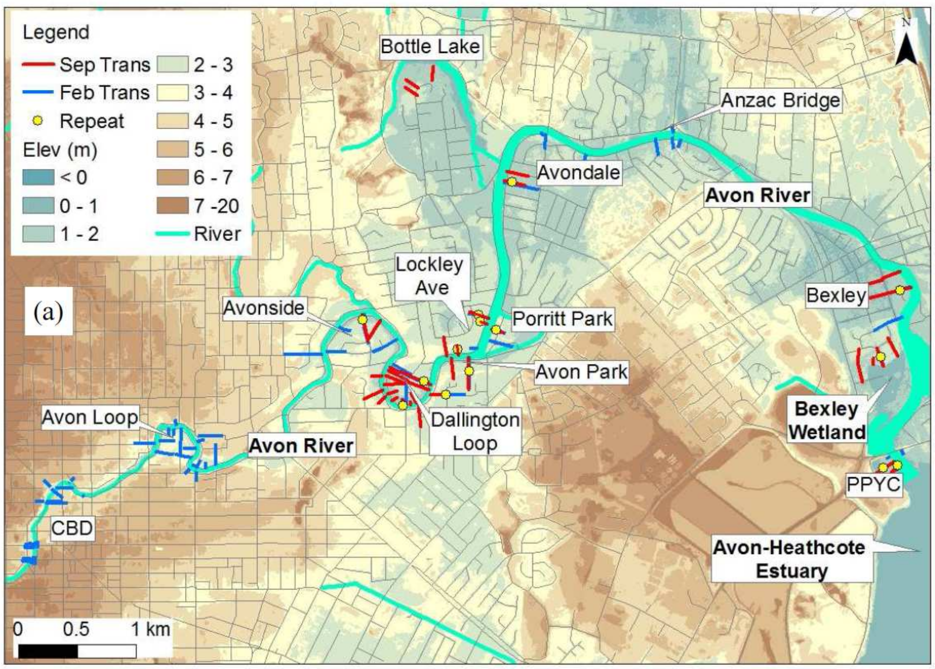

Figure 6. Location of transects for ground surveying measurements of lateral spreading along the Avon River (Robinson, 2015)

Table 1. Summary of river channel, ground slope and seismic demand characteristics at investigated transects shown in Figure 6

River Channel			Ground Slope	Conditional PGAs (g) normalized to M_w7.5[1)]		
Channel	**Overall range**	**Predominant range**	**θ (%)**	**Earthquake event**	**Overall range**	**Predominant range**
Height	1.5 m - 4.5 m	2.0 m - 4.0 m	θ < 1.0% at 50% of locations	Darfield (SEP2010)	0.17g – 0.18g	0.17g – 0.18g
Width	10 m - 60 m	20 m - 40 m	θ < 2.0% at 90% of locations	Christchurch (FEB2011)	0.28g – 0.38g	0.28g – 0.30g

[1)] Conditional peak ground accelerations (PGA) for conventional liquefaction assessment based on Bradley and Hughes (2012), normalized to magnitude 7.5 event.

Using acceleration records from a dense array of strong ground motion stations in Christchurch, Bradley and Hughes (2012) established conditional peak ground accelerations for conventional liquefaction assessment in Christchurch. These PGA values, normalized to a magnitude $M_w7.5$, and representative for the ground accelerations along the Avon River, are about 0.17 g – 0.18 g for the Darfield event, and are predominantly in the range between 0.28 g and 0.30 g for the Christchurch event, with some areas in the eastern part close to the estuary showing even higher accelerations. On average, along the Avon River, the seismic demand specific to liquefaction generated by the 2011 Christchurch earthquake was approximately twice that of the 2010 Darfield earthquake.

Observed Lateral Spreading Displacements Along the Avon River

Measured permanent horizontal ground displacements along transects on the Avon River are summarized in the first eight plots in Figure 7. The plots show the maximum magnitude of permanent spreading displacements at the river banks (L = 0 m), and also the distribution of ground displacements with the distance from the waterway (L) along the transect (i.e. perpendicular to the river). The plots are organized on an area basis, and show spreading features for eight areas along the Avon River, from the CBD towards the estuary (PPYC site).

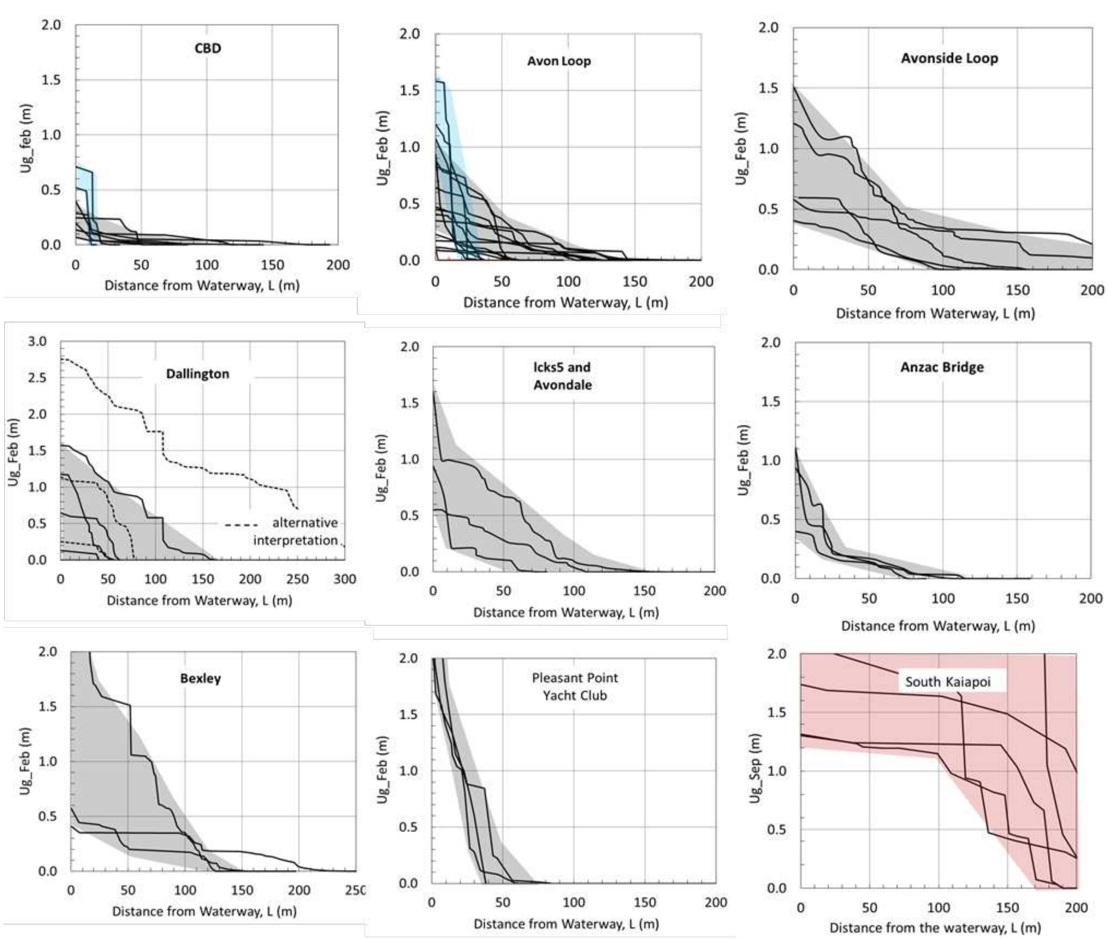

Figure 7. Permanent ground displacements along the Avon River (first eight plots) and in South Kaiapoi (last plot) obtained from ground surveying measurements (Robinson, 2015)

Measured lateral spreading displacements depicted in Figure 7 can be summarized as follows:

- Maximum permanent horizontal ground displacements at the banks of the Avon River are typically in the range between 0.5 m and 1.5 m. The magnitude of spreading displacements is generally smaller within the CBD, while largest displacements are observed at locations close to the estuary.
- The zone affected by spreading generally extends from the river banks up to about 150 m from the river. There are several locations at which the spreading is localized within a relatively narrow zone of 20 m to 40 m from the river (e.g. data highlighted in blue in Figure 7), while in few cases the zone affected by spreading extends to 200 m (or more) from the river.
- The spatial distribution of lateral ground displacements is highly variable indicating variability in lateral strains (stretch) and associated vertical offsets (differential settlements) within the zone affected by spreading.
- Finally, different distribution patterns in the ground displacements are evident in the different shapes of the U_g-L relationships. For example, the last plot shows a characteristic *block-mode* movement at South Kaiapoi, where the banks and adjacent ground to a distance of about 150 m from the stream moved as a rigid block (horizontal U_g-L relationships), and large cracks and ground fissures opened up at a distance of 120 m to 170 m, as represented by the steep nearly vertical segments in the U_g-L relationships. In this context, it is apparent that the spreading along the Avon River shows predominantly distributed pattern of ground displacements though some elements of block-type movement are also apparent at some locations.

Classification of Lateral Spreads

In order to further scrutinize the characteristics of lateral spreading displacements, the lateral spreads were classified into four different groups according to the magnitude of permanent ground displacements and their spatial distribution characteristics, as summarized in Figure 8. The first three groups simply reflect different magnitudes of maximum lateral displacements: (a) large displacements (generally close to 1 m or greater, with few exceptions); (b) moderate displacements (maximum displacements of approximately 0.5 m); and, (c) small displacements of less than 0.30 m (including in some cases negligible or no displacements). The fourth group identifies a special case of large magnitude displacements that are localized and significantly affect only a narrow zone of about 20 m to 40 m from the river.

Note that in the selection process for further investigation of lateral spreads, simple cases of lateral spreads were targeted where geotechnical data from CPT investigations were available. Hence, complex cases of lateral spreading, for which complex topographic features or meandering loop effects required significant interpretation of ground surveying measurements, were eliminated from these considerations. Also, relatively simple cases of lateral spreads but without supporting geotechnical data were not considered. On this basis, 25 cases were identified for further analysis, and these lateral spreads were classified into the four groups depicted in Figure 8.

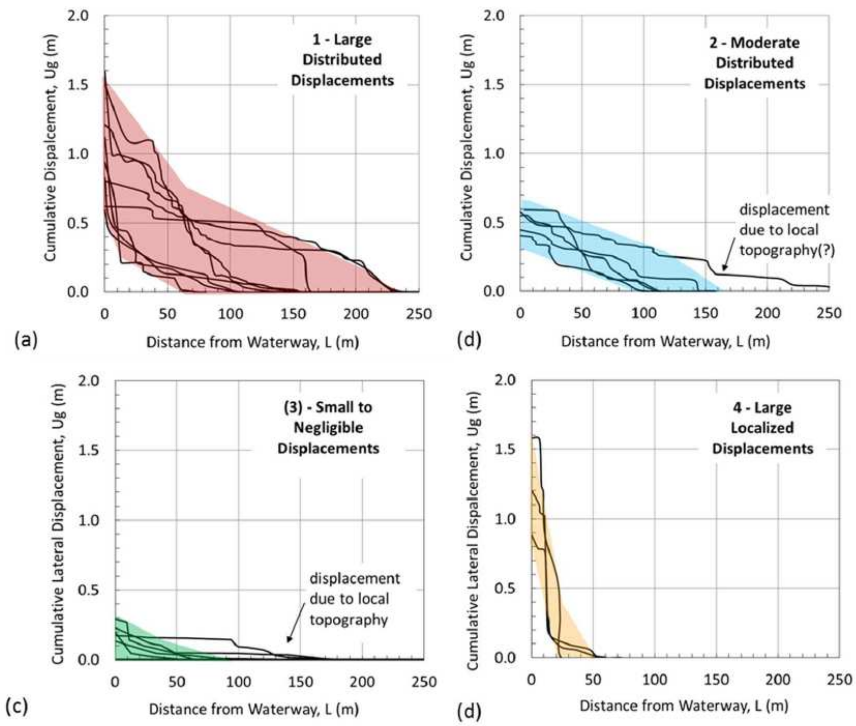

Figure 8. Classification of lateral spreads based on the magnitude of ground displacements: (a) large, (b) moderate and (c) small, and spatial distribution characteristics (d) large but localized spreading affecting a relatively narrow zone of 20 m to 40 m from the river (Robinson, 2015)

Geotechnical Analysis and Evaluation

The purpose of the geotechnical analysis and interpretation was to identify common characteristics, if any, for the lateral spreads manifesting large ground displacements, and in particular to understand the characteristics of soils and ground conditions, and potential critical layers for areas in which large lateral spreading displacements occurred. An additional objective was to identify important points of difference between the spreads with substantially different manifestation. For example, to identify differences in ground conditions between large and small lateral spreads, and hence indicate governing factors for lateral spreading from a slightly different perspective (i.e. using a different reference in the evaluation).

For each of the 25 selected transects, at least two CPTs were available in vicinity of the transect (typically within 25 m distance), one close to the river bank and another further away from the river. In addition, two to three other CPTs (or more) were used along (parallel to) and away from (perpendicular to) the river to evaluate spatial variability of soils and continuity of critical layers, in particular. On this basis, characteristic soil profiles including soil types, thickness of layers, and key soil parameters such as CPT tip resistance (q_c), soil behaviour type index (I_c), fines content (FC) and relative density (D_r) were identified. For each of the CPTs, liquefaction triggering analyses were then performed using three different methods proposed by Robertson and Wride (1998), Idriss and Boulanger (2008) and Boulanger and Idriss (2014), referred below as RW98, IB08, and BI14 respectively. In this way, factors of safety against liquefaction triggering were estimated along the transects of the investigated lateral spreads, for the 2010 Darfield earthquake and 2011 Christchurch earthquake.

Large-Displacement Lateral Spreads: Critical Layers

A soil profile for one of the CPTs along a transect where large ground displacements were observed is shown in Figure 9 to illustrate the characteristic soil profile and layer composition encountered at sites of large-displacement lateral spreads. As shown in the figure, there are three layers below the water table that are of particular importance in the lateral spreading evaluation: a silty soil (red) immediately below the water table, overlying a fine sand to silty sand (blue), and fine sand (green) layers. The three layers are sandwiched between a 1 m crust at the top and a dense sand layer at about 5 m depth. All layers have relatively low penetration resistances and hence high potential for liquefaction, as illustrated by the low CPT resistances, relative densities, and factors of safety against liquefaction triggering of less than 1.0.

Each of the seven transects of large-displacement lateral spreads was examined with regard to the characteristics of the three critical layers. As summarized in Figure 10, the following factors were comparatively examined for the seven sites: thickness of the layer (T_r), depth to top of layer (*z_top*), location of layer in relation to channel height (*z_top/H*), normalized tip resistance (q_{c1}), soil behaviour type index (I_c), normalized clean sand equivalent tip resistance (q_{c1Ncs}), and factor of safety against liquefaction triggering (FS_{liq}). Each of the three layers is shown with a symbol following the same colour code as in Figure 9. Hence, the blue symbols are related to the fine sand to silty sand layer shown in blue in Figure 9. Absence of a symbol for a given layer at a particular site indicates that the layer was not encountered at that site. While the presentation in Figure 10 is not very creative, it does allow for scrutiny of multiple parameters across the three different layers.

A close scrutiny of the data presented in Figure 10 shows that each of the three layers could contribute to liquefaction and lateral spreading, however the fine sand to silty sand layer (blue symbols) was identified as the critical layer with characteristics summarized in Figure 11. This layer was present at all seven sites exhibiting large-displacement lateral spreads, it was located at

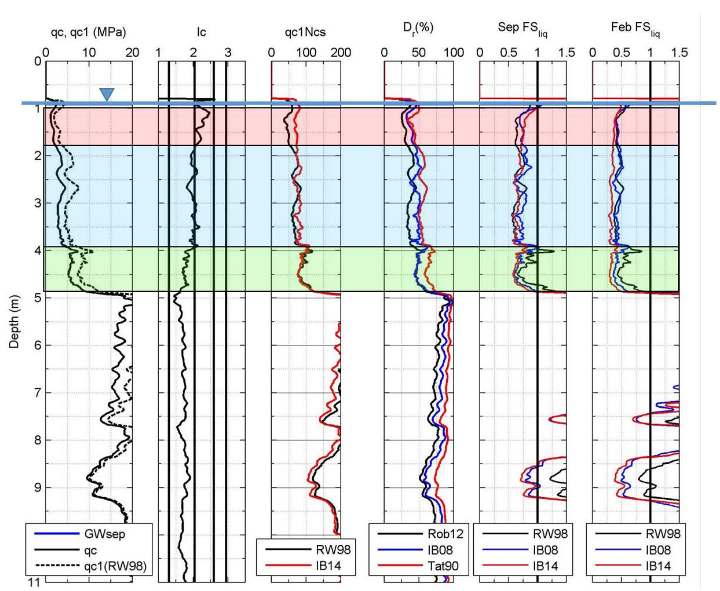

Figure 9. Characteristic soil profile and stratification encountered at large-displacement lateral spreads (Robinson, 2015)

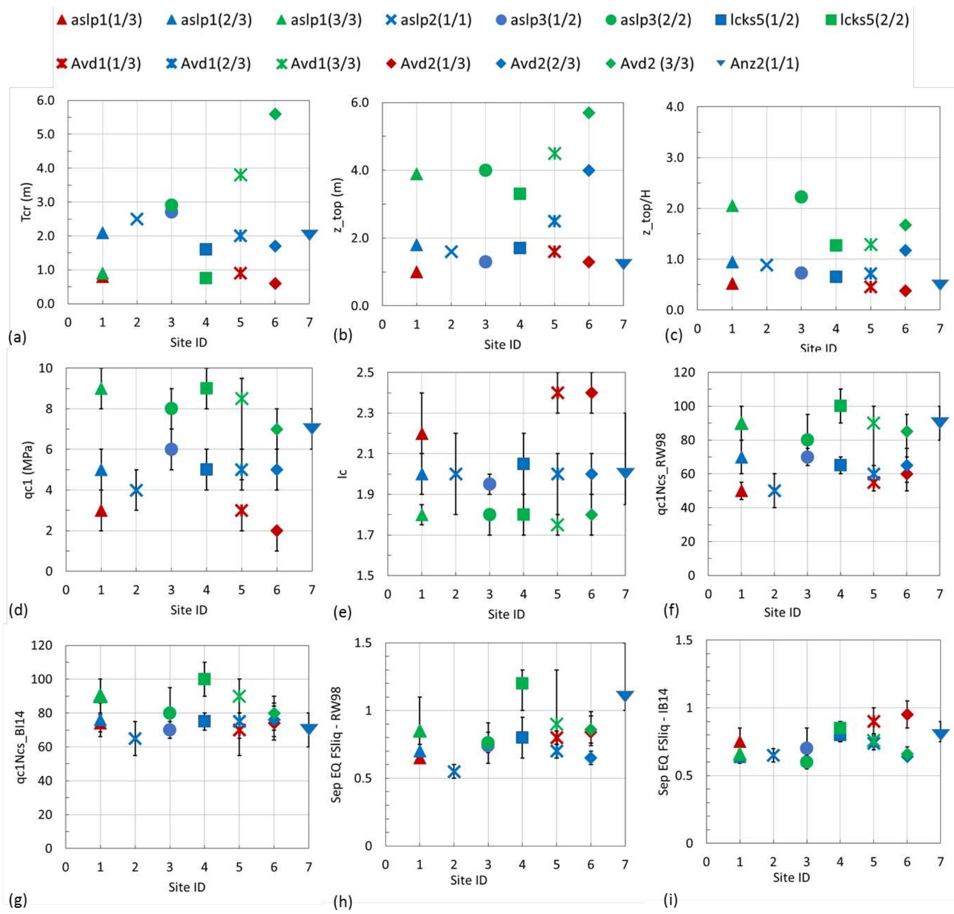

Tcr = thickness of critical layer (excludes non-liquefiable lenses and transition zones less than 10-20 cm); z_top = depth to top of critical layer, z_top/H = z_top divided by channel height, H; qc1 = tip resistance corrected for overburden pressure (RW98); Ic = soil behavior type index (RW98); qc1ncs = equivalent clean sand tip resistance (RW98, BI14); SepEQ-FS = factor of safety against liquefaction in the September earthquake (RW98, BI14)

Figure 10. Characteristics of potential critical layers for large-displacement lateral spreads (Robinson, 2015)

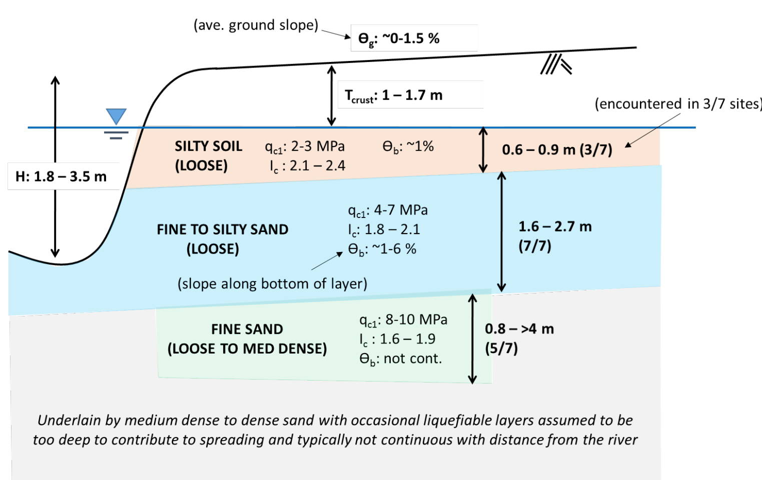

Figure 11. Characteristic soil profile of large-displacement lateral spreads (Robinson, 2015)

depths corresponding to the bottom of the river channel, and had consistently low equivalent clean sand normalized CPT tip resistance in the range between 55 and 75. The overlying silty soil was not encountered at several of the sites, while the underlying medium dense fine sand layer was localized near the river banks and was generally not encountered away from the river. It appears, however, that where present the underlying fine sand layer and overlying silty soil layer may have contributed to the liquefaction severity and consequent lateral spreading displacements through the substantial increase in the thickness of the liquefied zone as well as through sustained elevated excess pore water pressures and prolonged liquefaction-induced instability of soils.

Moderate-Displacement Lateral Spreads: Limited Thickness of Liquefied Soils

There are several important differences of the soil profile characteristics at moderate-displacement lateral spreads. First, the three-layer stratigraphy was generally not encountered, and commonly one or two of the three characteristic layers were absent at these sites. The fine sand to silty sand layer was encountered at only two of the five sites, and had thickness of 0.5 m and 1.0 m respectively. By and large, the cumulative thickness of the layers with high liquefaction potential was relatively small, and typically between 1.0 m and 1.5 m. Otherwise, the soil characteristics with regard to grain-size composition, density and penetration resistance were similar to those summarized in Figure 10, for the respective layers. Hence, the limited thickness of the liquefied layer appears to be the key reason for the reduced lateral spreading displacements at these sites.

Small-Displacement Lateral Spreads: Lack of or Discontinuous Critical Layers

The channel height, ground slope and seismic demand were generally similar at the large-displacement and small- or no-displacement lateral spreads. However, at six out of ten sites where negligible or no lateral spreading displacements were observed, none of the three characteristic layers with high liquefaction potential was encountered. As shown in Figure 12, at three of the remaining sites the critical fine sand to silty sand layer was very thin (less than 0.5 m thick), and importantly it was discontinuous both along the river and away from the river banks. These are critical features that resulted in small or no permanent ground displacements at these sites.

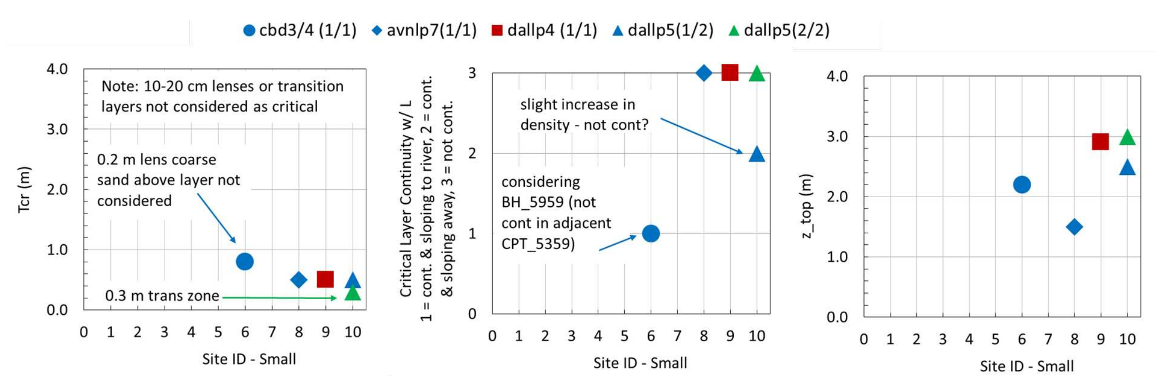

Figure 12. Absence of or discontinuity of critical layers at small- or no- displacement sites (Robinson, 2015)

Large-Displacement Localized Spreads: Critical Layer Localized Along the River Bank

The large-displacement localized lateral spreads were characterized by displacements of the river banks of 1.0 m to 1.5 m, which affected a narrow zone of about 20 m to 40 m from the river. There were only three such sites investigated, and at all of them an approximately 2 m thick layer of the fine sand to silty sand was encountered at or close to the river banks. However, the layer was not found at distances 40 m to 50 m away from the river. The presence of this layer in a narrow zone along the river, and its discontinuity with distance from the bank (and potentially along the bank as well) explains the localized nature of these spreads and confinement of deformation within a narrow spreading zone.

Conclusions

This paper has examined characteristics of lateral spreads caused in the 2010-2011 Canterbury earthquakes. It highlights the complexities of lateral spreading, but also the need for concurrent use of global and local surveying methods in the characterization of lateral spreads. The former depict global patterns in lateral spreading associated with topographic features, while the latter allow for effects associated with spatial variability of soils on a local scale.

Large-displacement lateral spreads occurred at sites characterized by a specific stratification involving three layers of silty soil, fine sand to silty sand, and fine sand respectively. All three layers (soils) have low liquefaction resistance, and are predicted to have liquefied during the 2010 Darfield and 2011 Christchurch earthquakes. The fine sand to silty sand layer was encountered at all sites of large-displacement lateral spreads, and was identified as the critical layer. This layer was characterized with low equivalent clean sand normalized CPT tip resistance (q_{c1Ncs}) of 55 to 75, thickness of about 2 m and location in the soil profile corresponding approximately to the bottom of the river channel. The particular three-layer stratigraphy increased the severity of liquefaction effects and consequent spreading displacements through both increase in the thickness of the liquefied zone and prolonged duration of liquefaction effects.

Moderate-displacement lateral spreads occurred at sites where the three-layer stratigraphy was not prevalent and cumulative thickness of layers with low liquefaction resistance was about 1.0 m to 1.5 m. At sites where either small-displacement lateral spreads or no displacements were observed, the critical layers were either absent, or very thin (less than 0.5 m thick) and discontinuous both along the river and away from the river banks. The importance of lateral continuity of critical layers was also evident in the case of large-displacement localized lateral spreads in which narrow zone of spreading along the river was associated with critical layers confined within a narrow zone along the river banks.

The findings of this study and methodology used in the characterization of lateral spreads elucidate alternative approaches to evaluation of lateral spreading in which particular features such as maximum magnitude and spatial distribution of spreading displacements are examined through scrutiny of factors that have governing influence on these spreading characteristics.

Acknowledgments

The principal support for this study was provided by grants from the New Zealand Earthquake Commission (EQC) and Natural Hazards Research Platform (NHRP). The second author would like to acknowledge the scholarships provided by the University of Canterbury, New Zealand Geotechnical Society and EQC. The contribution of a large number of undergraduate and postgraduate students in the field reconnaissance efforts is also acknowledged. The first phase (September-October 2010) of these efforts was financially supported by the University of Canterbury (UC) and EQC. The second phase of reconnaissance (November 2010-Februrary 2011) was a joint summer research program of UC and the University of Auckland (UA), which was partially funded by the Environment Canterbury (ECan). The third phase (February 2011 – May 2011) involved the efforts of UC postgraduates as part of the February earthquake reconnaissance.

References

Boulanger, R. W., and Idriss, I. M. 2014. *CPT and SPT based liquefaction triggering procedures*. Report No. UCD/CGM-14/01, University of California, Davis, CA, 134 pp.

Bradley, B.A. & Hughes, M. 2012. Conditional *Peak Ground Accelerations in the Canterbury Earthquakes for Conventional Liquefaction Assessment*. Technical Report Prepared for the Department of Building and Housing.

Brown, L.J. & Weeber, J.H. 1992. *Geology of the Christchurch Urban Area*. Lower Hutt, New Zealand: Institute of Geological and Nuclear Sciences CGD (2013).

CGD 2013. "*Liquefaction and Lateral Spreading Observations*", Map Layer CGD0300 - 11 Feb 2013, retrieved February 2014, from https://canterburygeotechnicaldatabase.projectorbit.com/.

CGD 2014. "*Event Specific Groundwater Surface Elevations*", Map Layer CGD0800 - 12 June 2014, retrieved July 2014 from https://canterburygeotechnicaldatabase.projectorbit.com/.

Cubrinovski, M. and McCahon, I. 2011. *Foundations on Deep Alluvial Soils*, report prepared for the Canterbury Earthquakes Royal Commission, 40 pp.

Cubrinovski, M., Robinson, K., Taylor, M., Hughes, M., & Orense, R. 2012. Lateral spreading and its impacts in urban areas in the 2010-2011 Christchurch earthquakes. *New Zealand Journal of Geology and Geophysics*, 55(3), 255-269.

Idriss, I.M. & Boulanger, R.S. 2008. *Soil Liquefaction during Earthquakes*. Oakland, CA: Earthquake Engineering Research Institute.

Ishihara, K., Yoshida, K., & Kato, M. 1997. Characteristics of Lateral Spreading in Liquefied Deposits during the 1995 Hanshin-Awaji Earthquake. *Journal of Earthquake Engineering*, 1(1), 23-55.

Robertson, P.K. & Wride, C.E. 1998. Evaluating cyclic liquefaction potential using the cone penetration test. *Can. Geotech. J.*, Vol. 35: 442-459.

Robinson, K. 2015. *Liquefaction-Induced Lateral Spreading in the 2010-2011 Canterbury Earthquakes*. PhD Thesis, University of Canterbury (in print).

Tonkin & Taylor 2015. LiDAR Data Interpretation. Preliminary data shared by Tonkin &Taylor.